Electrochemically controlled cocrystallisation of caffeine:1-hydroxy-2-naphthoic acid

Magdalena Kaliszczak, [1] Pierrick Durand, [2] Emmanuel Wenger, [2] Manuel Dossot, [1] Franca Jones, [3] Damien W. M. Arrigan, [3*] Grégoire Herzog[1*]

1: Université de Lorraine, CNRS, LCPME, F-54000 Nancy, France

2: Université de Lorraine, CNRS, CRM2, F-54000 Nancy, France

3: School of Molecular and Life Sciences, Curtin University, GPO Box U1987, Perth, Western Australia 6845, Australia

*: D.Arrigan@curtin.edu.au; gregoire.herzog@univ-lorraine.fr

This document is a postprint. Final version has been published in *CrystEngComm*, 2022, DOI: 10.1039/D1CE01281A

Controlled formation of cocrystals is an important objective in drug development. Here, cocrystallisation of caffeine and 1-hydroxy-2-naphthoic acid was investigated at the interface between two immiscible electrolyte solutions under chemical polarisation. In this way, selective cocrystallisation was achieved, as verified by X-ray diffraction and Raman spectroscopy. Positive interfacial potentials favoured the formation of one polymorphic form of caffeine:1-hydroxy-2-naphthoic acid cocrystal. This approach to electrochemically controlled cocrystallisation opens up new possibilities for drug development.

The search for innovative crystallisation methods is a subject of constant interest as most drugs appear as crystalline forms whose polymorphs may have different toxicity, hygroscopicity or physical and chemical stability.[1–3] An additional issue encountered in drug development is the low stability in humid environments

of the solid active pharmaceutical ingredients (APIs), resulting in manufacturing and storage problems.[4] A drug cocrystal is a class of pharmaceutical substance which can improve these properties. Pharmaceutical cocrystals may contain two or more guest molecules recognized as safe (e.g. preservatives, excipients, carboxylic acids) or another drug incorporated with the API in the crystal lattice in definite stoichiometric amounts, without affecting the pharmacological activity of the drug.[5–7] Cocrystals can be formed by non-covalent interactions (e.g. hydrogen bonds) between functional groups such as carboxylic acid-amide and alcohol-pyridine.[8] Caffeine is a purine alkaloid, which has a stimulating effect on the nervous system and is used to reinforce analgesic and antipyretic drugs action.[4] This component is unstable in a humid environment and tends to change into unstable hydrates.[9] Therefore, caffeine is often used as a model compound in cocrystal studies with carboxylic acids, since such cocrystals are known to improve its physical properties.[4,10] Several solvent based methods are used to form cocrystals: e.g. solvent evaporation, solvent cooling, cocrystallisation from melt, different types of grinding and slurrying, anti-solvent cocrystallisation,[11] and liquid-liquid crystallisation.[12] Recent studies have shown that an electric field applied across a biphasic system of miscible solvents resulted in the formation of organic crystals[13] and metal organic frameworks.[14] We propose here the cocrystallisation of caffeine with organic carboxylic acids at the interface between two immiscible electrolyte solutions (ITIES). The transfer of ionic species through the ITIES is caused by the application of an electrical potential difference, which can be controlled either by a potentiostat[15] or by dissolution of a common ion in each phase.[16] Electrochemistry at the ITIES has been harnessed in recent years for the electrogeneration of a variety of materials such as Au nanoparticle assemblies,[17] amorphous mesoporous silica,[18] porphyrin films,[19,20] protein deposits,[21,22] and polymer films.[23] A potential difference, $\Delta_o^w \phi$, was applied across the oil-water interface. This driving force triggered a charge transfer, either ion or electron transfer, across the interface and led to material electrodeposition at the interface. We have investigated here the control of cocrystallisation of two reagents of mismatch solubility by the imposed potential difference at the oil-water interface. The system comprised caffeine (Caff) as a hydrophilic compound present in the aqueous phase and 1-hydroxy-2-naphthoic acid (1H2N) as a coformer present in the oil phase, 1,2-dichloroethane (DCE).

The effect of chemical polarisation of the oil-water interface on the polymorphism of the cocrystals formed was also explored.

Caff:1H2N cocrystals were formed at a water-oil interface by preparing a series of vials of varying experimental conditions (Figure 1). Aqueous solutions contained 10 mM LiCl and Caff concentrations of 10 mM, 30 mM or saturated. The organic phase contained 10 mM 1H2N and KTPBCl (potassium tetrakis(4-chlorophenyl) borate) or BACl (Bis(triphenylphosphoranylidene)ammonium chloride) salts dissolved in 1,2-dichloroethane (1,2-DCE), which impose a potential difference ($\Delta_o^w \phi$) across the ITIES.[24,25]

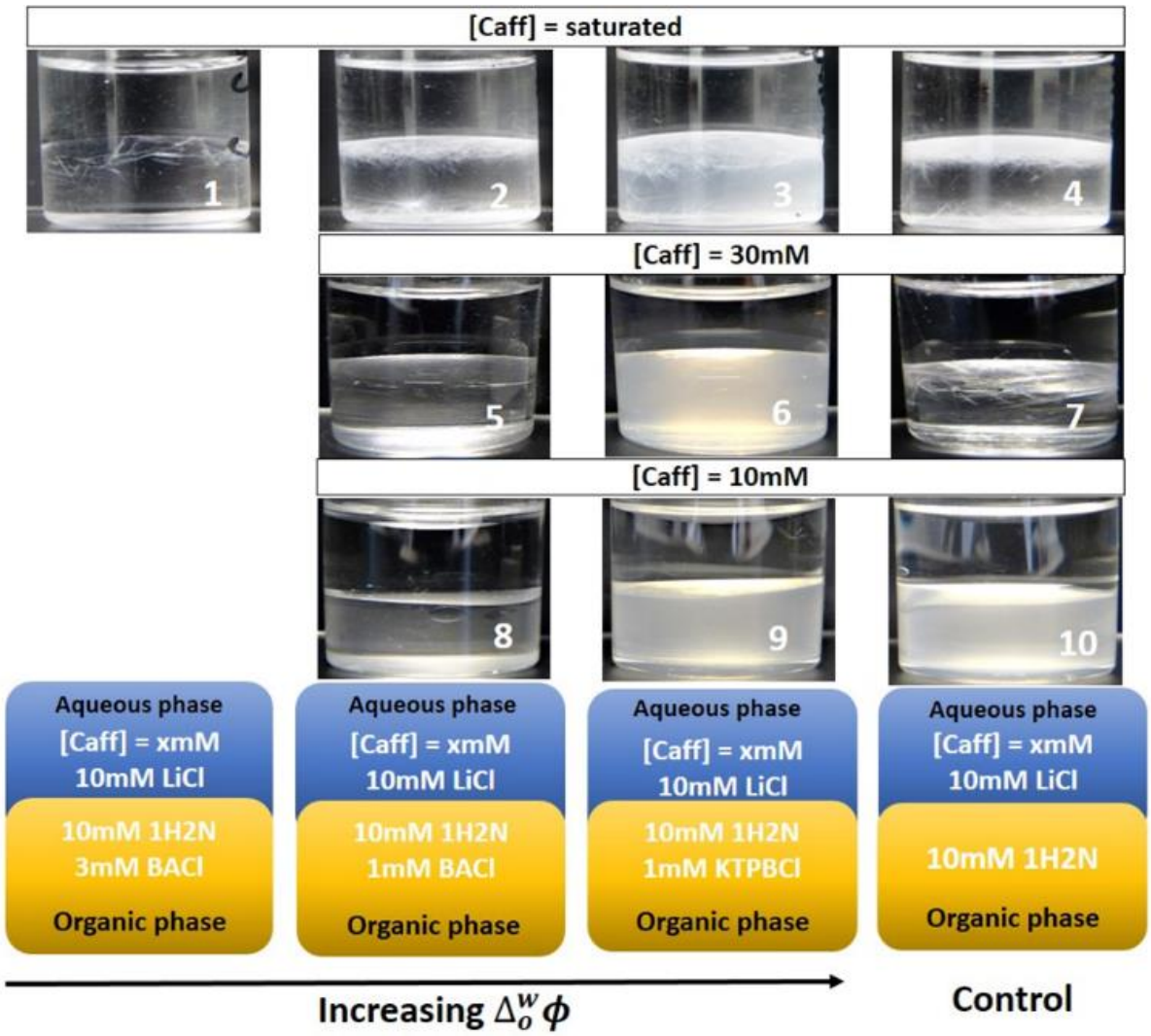

Figure 1. (A) Photographs of aqueous-1,2-DCE biphasic systems for various Caffe concentrations and various interfacial polarisations after the vials were left for 16 h at room temperature. (B) Corresponding experimental conditions.

The $\Delta_o^w\phi$ imposed is lower at the left-hand side and increases towards positive potentials towards the right. Control experiment vials (Fig 1 Vials 4, 7, 10) were obtained in the absence of potential-imposing salts in the organic phase. When caffeine was at saturation in the aqueous phase, the low interfacial $\Delta_o^w\phi$ hindered the transfer of caffeine from the aqueous to the organic phase (Fig 1 Vial 1), whereas the observed quantity of crystals increased with the interfacial $\Delta_o^w\ \phi$ (Fig 1 Vial 2 and 3). A high interfacial $\Delta_o^w\ \phi$ favoured the transfer of cationic $CaffH^+$ from aqueous to organic.[26] Cyclic voltammograms showed that $CaffH^+$ is reversibly transferring at $\Delta_o^w\ \phi^{1/2}$ = 0.39V (Fig S1). In vial experiments, the transfer of $CaffH^+$ caused supersaturated conditions in the organic phase, resulting in cocrystallisation with 1H2N. The effect of interfacial polarisation on the cocrystallisation process was also noticeable at lower caffeine concentrations. For 30 mM (Fig 1 Vial 5) and 10 mM (Fig 1 Vial 8) of Caff, the formation of cocrystals was

inhibited at the intermediate potential. At higher interfacial polarisation and [Caff] = 10 mM, it was possible to collect cocrystals located at the interface what was not possible in control experiment (Fig 1 Vial 10). These results suggest that the cocrystallisation of Caff: 1H2N can be controlled by the tuning of the interfacial potential. Indeed, the blurred organic phase for [Caff] = 10 mM, is attributed to the formation of Caff: 1H2N precipitates, this is in contrast with the clear organic phase when vials were initially set up (Fig S2).

The cocrystals, formed in biphasic systems reported in Fig 1, were collected and analysed by scanning electron microscopy (SEM) (Fig S3-4-5). In the case of saturated Caff, the largest crystals were obtained for the intermediate $\Delta_o^w \phi$ (Fig S3 Vial 2), with crystal sizes (426 ± 42) µm, whereas cocrystals obtained with the highest $\Delta_o^w \phi$ were (121 ± 11) µm and those obtained with the control experiment were (50 ± 3) µm. This indicated an influence of the $\Delta_o^w \phi$ on Caff mass transport and hence on the size of the cocrystals. For 30 mM Caff, no precipitation was observed for the intermediate $\Delta_o^w \phi$. The crystal size decreased when the $\Delta_o^w \phi$ increased (32 ± 1 µm for the highest $\Delta_o^w \phi$, whereas the crystal size for the control conditions was 47 ± 3 µm). It was not possible to collect the precipitate for the control experiment of 10 mM concentration of caffeine and hence there is no analysis by SEM.

Cocrystals were analysed by single crystal X-ray diffraction (XRD). Multiple single crystal measurements showed either phase I or phase II (Fig S5), which corresponded with the Caff: 1H2N cocrystals already published in the Cambridge Crystallographic Data Centre (CCDC)[27] (Table S2 Fig S5). Such complexes crystallized in the monoclinic P21/n space group with a stoichiometric amount of Caff and 1H2N. Caff and 1H2N interacted by hydrogen bonding between the carbonyl and imidazole groups.[9] Single crystal diffractograms were completed with powder XRD for a more representative analysis of the sample. Phase I, phase II, and a small impurity coming from caffeine powder were found in all samples. None of the other salts of the chemicals initially present were visible by powder XRD, nor was there a 1H2N residue. All the diffraction peaks were therefore well fitted and only indexed by phase I, phase II and caffeine. Polarisation of the interface was found to favour phase I over the phase II. Indeed, analyses of the collected powders by X-ray diffraction for 30 mM (Fig S6) and Caff saturated concentration (Fig 2) showed that phase I was predominant in the sample when the interface was positively polarised, whereas phase II was more present in the control sample. Similar results were obtained for a saturated solution of caffeine. Under the influence of interfacial polarisation, almost exclusively phase I was obtained. In the case of high concentration of caffeine, we also saw a larger caffeine residue (Fig 2).

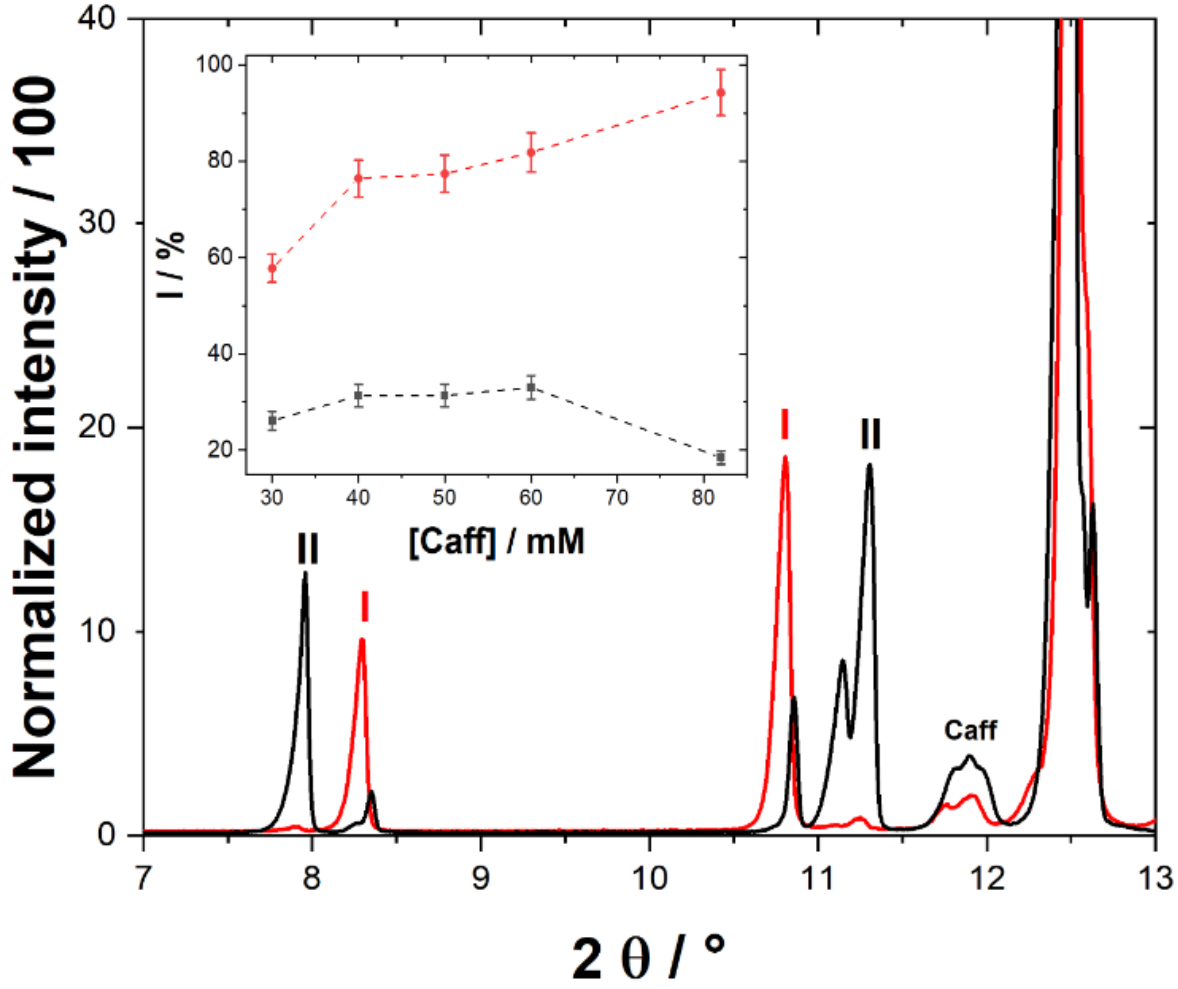

Figure 2: Diffractograms of cocrystal (Caff: 1H2N) powders in biphasic systems at high $\Delta_o^w \phi$ (red) and in control experiments (black). Peaks were attributed to crystallographic phase I or II. Caff corresponds the residual starting material. Inset: Phase I % as a function of [Caff] at high $\Delta_o^w \phi$ (red) and for control experiments (black).

Based on the CCDC files, we could estimate the diffractograms the proportion of a phase I and II in the collected crystals. Powder diffraction patterns of pure single-phase material were simulated from the known structures. The proposed calculations are semi-quantitative and their main purpose was to compare the phase proportions of the test samples. The intensity of the peaks in analysed samples has been normalised and compared with the normalised intensity of the pure single phases from the simulated spectrum of phase I and II. The predominance of phase I rose with increasing caffeine concentration in the aqueous phase when the interface was positively polarised, which was not the case in the control

experiments (Inset Fig 2). Additionally, the content of unreacted caffeine is lower when a high $\Delta_o^w \phi$ was applied (Fig S7).

Cocrystals were analysed by Raman spectroscopy to complement the information obtained by crystallography. A typical Raman spectrum of cocrystals is shown in Fig 3 for the 1100 – 1800 cm^{-1} region. Full Raman spectra are shown in Fig S8. Samples were analysed at three different locations in order to obtain statistically relevant information of the sample composition. Raman peaks were attributed using the theoretical spectrum calculated by density functional theory (Fig S9). The two most prominent peaks of cocrystals were observed at 1378 cm^{-1} and 1648 cm^{-1}. The shift of the peak at 1378 cm^{-1} compared to pure caffeine is caused by the hydrogen bond between the imidazole ring of the caffeine and the carboxylic group of 1H2N,[4,28] whereas the Raman shift of the peak at 1648 cm^{-1} is assigned to the C=O stretching peak involved in the intermolecular hydrogen bond in the naphthoic acid.[29]

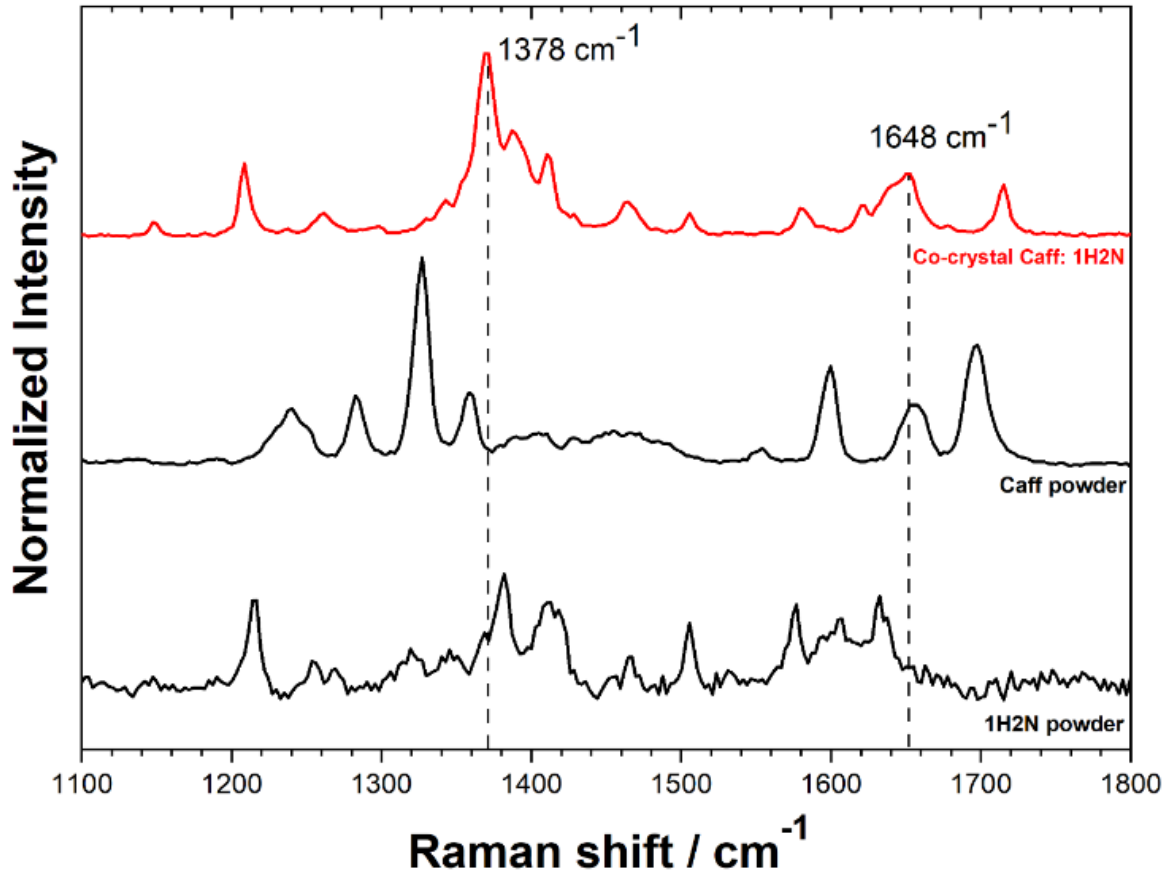

Figure 3: Raman spectra for Caff: 1H2N cocrystals (obtained with caffeine saturated aqueous phase and at high positive polarization), caffeine and 1H2N. Full spectra shown in Fig S8-S9.

Raman spectra showed a noticeable difference in the characteristic bands between the Caff: 1H2N cocrystals and the reagents, confirming that the initial materials were not present in the product collected

from the interface. The shifts obtained in the region 1300 – 1800 cm^{-1} are characteristic for the 1:1 complex involving hydrogen bonds between the two molecules which are consistent with the XRD analysis.[9] The comparative Raman spectra analysis showed that the same bands were obtained, regardless of the experimental conditions (Fig S8) highlighting the consequences of hydrogen bond formation in the cocrystals leads to the same shifts, although cocrystals were obtained in form I or form II depending on the crystallisation conditions. This range of Raman wavenumbers is therefore not sensitive to the different molecular arrangement of these two forms.

In the absence of polarisation, $CaffH^+$ and 1H2N are cocrystallising through an interfacial process (Fig 4). When the interface is polarised with a sufficiently high potential, $CaffH^+$ is transferred to the organic phase, forming a complex with 1H2N and releasing a proton. Indirect evidence of the $CaffH^+$ transfer upon chemical polarization of the interface was demonstrated by SEM analysis of the content of the organic phase (Fig S10). Large crystals are collected from the organic phase when the interface was positively polarized. When the interface is polarized with an intermediate or a negative potential difference, almost no deposits are observed. The fate of protons resulting from the cocrystallisation of Caff:1H2N is investigated by measuring the pH of the aqueous phase before and after experiments (Fig S11). The formation of molecular cocrystals, rather than ionic cocrystals of cationic Caff and anionic 1H2N is supported by the absence of peaks related to carboxylate in the Raman spectrum (Fig 3). At high $\Delta_o^w\phi$, the pH increases after cocrystallisation, suggesting that H^+ remained in the organic phase. This is assigned to an interfacial $\Delta_o^w\phi$ greater than the standard interfacial transfer potential of H^+ ($\Delta_o^w\phi > \Delta_o^w\phi_{H^+}^0$)[30]. On the contrary, in the absence of polarisation or in the case of low interfacial $\Delta_o^w\phi$, the interfacial $\Delta_o^w\phi$ favours the presence of protons in the aqueous phase ($\Delta_o^w\phi < \Delta_o^w\phi_{H^+}^0$), resulting in a decrease in pH.

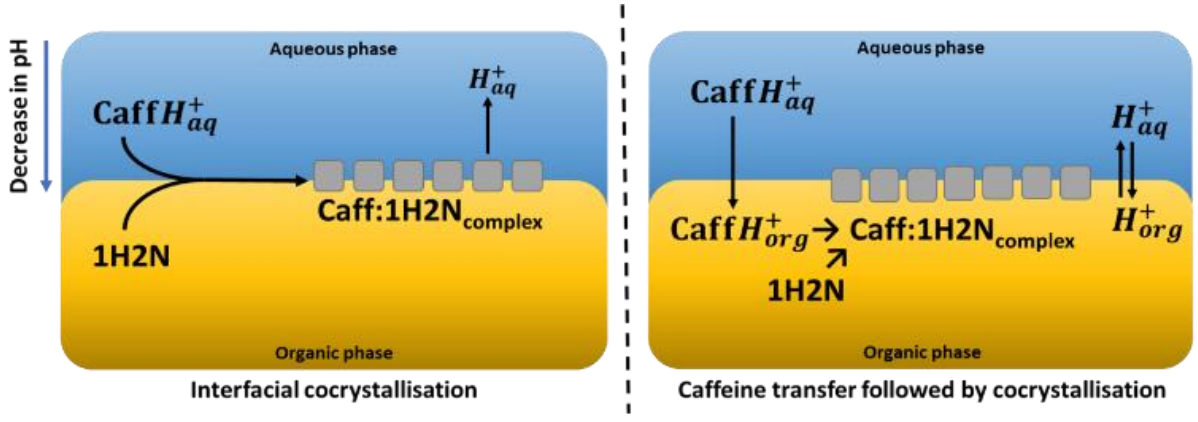

Figure 4: Schematic representations of the mechanism of interfacial cocrystallisation (left) and of $CaffH^+$ transfer to the organic phase followed by cocrystallisation in the organic phase.

Conclusions

Cocrystals of two reagents of mismatch solubility, hydrophilic Caff and lipophilic 1H2N, were obtained at a water-oil interface. Polarisation of this interface allowed the electrochemical control of the cocrystallisation process. XRD and Raman spectroscopy confirmed that the products collected at the water-oil interface were molecular cocrystals of caff: 1H2N, free of starting reagents and solvents. XRD analysis showed that for non-polarised interfaces, a mixture of phase I and II cocrystals were obtained, whereas cocrystals of phase I were formed when a high interfacial $\Delta_o^w \phi$ was applied. The difference of predominant polymorph in the absence or in the presence of interfacial polarisation is attributed to the different cocrystallisation mechanisms. Interfacial cocrystallisation is dominating in the absence of polarisation, whereas cocrystallisation is occurring in the organic phase at high $\Delta_o^w \phi$.

Polarisation of the water-oil interface offers a control of the localisation of cocrystallisation (organic vs interfacial) and the reagents concentration distribution across this interface. This feature is a valuable addition to the vast combination of APIs, coformers and solvent. The electrochemically controlled cocrystallisation would be applicable to many pharmaceutical compounds.

Acknowledgements

References

1 D. P. Elder, R. Holm and H. L. de Diego, *Int. J. Pharm.*, 2013, **453**, 88–100.

2 W. Jones, W. D. S. Motherwell and A. V. Trask, *MRS Bull.*, 2006, **31**, 875–879.

3 T. S. Thakur and R. Thakuria, *Cryst. Growth Des.*, 2020, **20**, 6245–6265.

4 A. V Trask, W. D. S. Motherwell and W. Jones, *Cryst. Growth Des.*, 2005, **5**, 1013–1021.

5 N. Qiao, M. Li, W. Schlindwein, N. Malek, A. Davies and G. Trappitt, *Int. J. Pharm.*, 2011, **419**, 1–11.

6 E. Grothe, H. Meekes, E. Vlieg, J. H. ter Horst and R. de Gelder, *Cryst. Growth Des.*, 2016, **16**, 3237–3243.

7 N. K. Duggirala, M. L. Perry, Ö. Almarsson and M. J. Zaworotko, *Chem. Commun.*, 2016, **52**, 640–655.

8 A. Karagianni, M. Malamatari and K. Kachrimanis, *Pharmaceutics*, 2018, **10**, 1–30.

9 D.-K. Bučar, R. F. Henry, X. Lou, R. W. Duerst, T. B. Borchardt, L. R. MacGillivray and G. G. Z. Zhang, *Mol. Pharm.*, 2007, **4**, 339–346.

10 R. Thakuria, M. Arhangelskis, M. D. Eddleston, E. H. H. Chow, K. K. Sarmah, B. J. Aldous, J. F. Krzyzaniak and W. Jones, *Org. Process Res. Dev.*, 2019, **23**, 845–851.

11 M. Karimi-Jafari, L. Padrela, G. M. Walker and D. M. Croker, *Cryst. Growth Des.*, 2018, **18**, 6370–6387.

12 S. J. Diez, M. D. Eddleston, M. Arhangelskis, M. Milbled, M. J. Müller, A. D. Bond, D.-K. Bučar and W. Jones, *Cryst. Growth Des.*, 2018, **18**, 3263–3268.

13 F. M. Maddar, D. Perry and P. R. Unwin, *Cryst. Growth Des.*, 2017, **17**, 6565–6571.

14 P. D. Morris, I. J. McPherson, M. A. Edwards, R. J. Kashtiban, R. I. Walton and P. R. Unwin, *Angew. Chemie Int. Ed.*, 2020, **59**, 19696–19701.

15 Z. Samec, *Pure Appl. Chem.*, 2004, **76**, 2147–2180.

16 G. Luo, S. Malkova, J. Yoon, D. G. Schultz, B. Lin, M. Meron, I. Benjamin, P. Vanýsek and M. L. Schlossman, *J. Electroanal. Chem.*, 2006, **593**, 142–158.

17 E. Smirnov, P. Peljo, M. D. Scanlon and H. H. Girault, *ACS Nano*, 2015, **9**, 6565–6575.

18 L. Poltorak, G. Herzog and A. Walcarius, *Electrochem. Commun.*, 2013, **37**, 76–79.

19 A. F. Molina-Osorio, D. Cheung, C. O'Dwyer, A. A. Stewart, M. Dossot, G. Herzog and M. D. Scanlon, *J. Phys. Chem. C*, 2020, **124**, 6929–6937.

20 A. F. Molina-Osorio, J. A. Manzanares, A. Gamero-Quijano and M. D. Scanlon, *J. Phys. Chem. C*, 2020, **124**, 18346–18355.

21 G. Herzog, V. Kam and D. W. M. Arrigan, *Electrochim. Acta*, 2008, **53**, 7204–7209.

22 B. R. Silver, V. Fülöp and P. R. Unwin, *New J. Chem.*, 2011, **35**, 602–606.

23 K. Kowalewska, K. Sipa, A. Leniart, S. Skrzypek and L. Poltorak, *Electrochem. Commun.*, 2020, **115**, 106732.

24 T. Iwata, H. Nagatani and T. Osakai, *Anal. Sci.*, 2017, **33**, 813–819.

25 L. Quoc Hung, *J. Electroanal. Chem.*, 1980, **115**, 159–174.

26 L. Poltorak, I. Eggink, M. Hoitink, E. J. R. Sudhölter and M. de Puit, *Anal. Chem.*, 2018, **90**, 7428–7433.

27 C. R. Groom, I. J. Bruno, M. P. Lightfoot and S. C. Ward, *Acta Crystallogr. Sect. B Struct. Sci. Cryst. Eng. Mater.*, 2016, **72**, 171–179.

28 F. Ucun, A. Sağlam and V. Güçlü, *Spectrochim. Acta Part A Mol. Biomol. Spectrosc.*, 2007, **67**, 342–349.

29 M. Inoue, T. Osada, H. Hisada, T. Koide, T. Fukami, A. Roy, J. Carriere and R. Heyler, *Anal. Chem.*, 2019, **91**, 13427–13432.

30 I. Hatay, B. Su, F. Li, R. Partovi-Nia, H. Vrubel, X. Hu, M. Ersoz and H. H. Girault, *Angew. Chemie - Int. Ed.*, 2009, **48**, 5139–5142.